Synlett S. M. Barbon et al. Letter

An Azide-Functionalized Nitronyl Nitroxide Radical: Synthesis, Characterization and Staudinger–Bertozzi Ligation Reactivity

Stephanie M. Barbon[a,1]
Pierangelo Gobbo[a,1]
Wilson Luo[a]
Jacquelyn T. Price[a]
Mark C. Biesinger[b]
Mark S. Workentin*[a]
Joe B. Gilroy*[a]

[a] Department of Chemistry and the Centre for Advanced Materials and Biomaterials Research (CAMBR), The University of Western Ontario, 1151 Richmond St. N., London, ON, N6A 5B7, Canada
mworkent@uwo.ca, joe.gilroy@uwo.ca
[b] Surface Science Western, The University of Western Ontario, 999 Collip Circle, London, ON, N6G 0J3, Canada

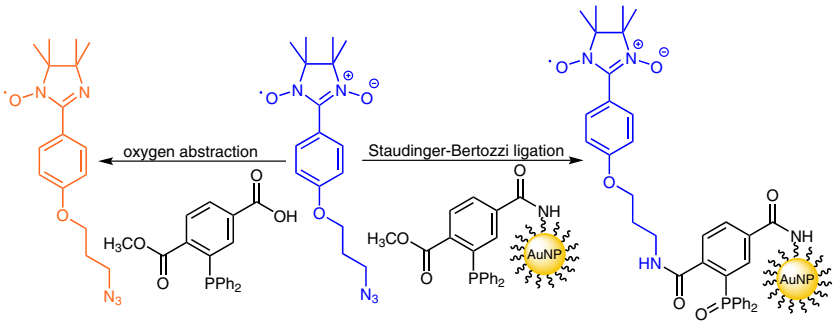

Received: 31.07.2015
Accepted after revision: 15.09.2015
Published online: 14.10.2015
DOI: 10.1055/s-0035-1560707; Art ID: st-2015-r0603-l

Abstract An azide-functionalized nitronyl nitroxide was synthesized and its reactivity towards the Staudinger–Bertozzi ligation was explored. Whereas a model reaction in solution showed the conversion of nitronyl nitroxide to an imino nitroxide radical, the same reaction at the interface of gold nanoparticles allowed for successful covalent incorporation of the nitronyl nitroxide radical onto the nanoparticles.

Key words gold nanoparticles, stable radicals, nitronyl nitroxides, bioorthogonal chemistry, EPR spectroscopy, X-ray spectroscopy

Since the discovery of the persistent triphenylmethyl radical **1** by Gomberg in 1900,[2] scientists have been intrigued by the chemistry of stable radicals. Stable radicals have found application in a variety of fields[3] including as organic magnetic materials,[4] MRI contrast agents,[5] and as the redox-active component of organic radical batteries.[6] One of the most well studied classes of stable radicals are the nitroxide radicals, which include 2,2,6,6-tetramethylpiperidine-1-oxyl (TEMPO; **2**) and the resonance-delocalized nitronyl nitroxides **3** (Figure 1).

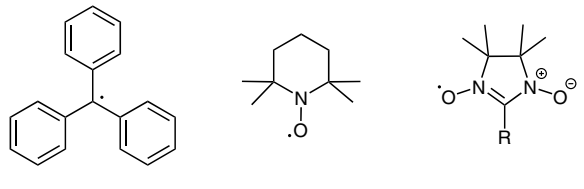

Figure 1 Examples of stable radical species

Nitronyl nitroxides and nitroxide radicals have been used for a variety of applications, including in organic synthesis for the abstraction of hydrogen atoms and the oxidation of alcohols and sulfides.[7] Another interesting application of this class of radicals is their use as radical scavenging agents.[8] This trait has led to many applications including scavenging of protein-based radicals,[9] reactive oxygen and nitrogen species in the body[10] and nitric oxide.[11] One of the most common uses of this phenomenon is in nitroxide-mediated polymerization, which is a common controlled radical polymerization reaction.[12] These radicals are also used for spin labeling, which involves introducing radicals into biological systems or macromolecules and monitoring their location and local environment by using electron paramagnetic resonance (EPR) spectroscopy, a non-invasive and non-destructive technique. These radicals specifically are favored because of their stability in a variety of solvents and over a wide pH range, and because of the ease with which they can be synthetically modified for a specific target.[13] Decoration of nanoparticles and carbonaceous nanomaterials with stable radicals is also an area of significant interest.[14]

Given the variety of applications of nitroxide and nitronyl nitroxide radicals, the development of facile methods for appending these radicals onto different materials (i.e., nanoparticles, polymers, biomolecules, etc.) is desirable.[15] Herein, we report the synthesis of an azide-substituted nitronyl nitroxide radical, which benefits from resonance delocalization and is expected to have enhanced stability relative to similar azide-TEMPO radicals.[16] Furthermore, as a proof of concept, we explore its interfacial reactivity through the Staudinger–Bertozzi ligation reaction.

The 4-(3-azidopropoxy) substituted 1,3-dihydroxy-4,4,5,5-tetramethyl-2-phenylimidazolidine **4** was synthesized from 4-(3-azidopropoxy)benzaldehyde[17] and *N*,*N*′-dihydroxy-2,3-dimethyl-2,3-butanediamine[18] and fully characterized by ^{1}H and ^{13}C NMR spectroscopy (Figures S1 and S2 in the Supporting Information), mass spectrometry, and elemental analysis.[19] Lead oxide was used to oxidize imidazolidine **4** to the azide-functionalized nitronyl nitroxide **5** (Scheme 1). To our knowledge, **5** is the first example of an azide-functionalized nitronyl nitroxide.

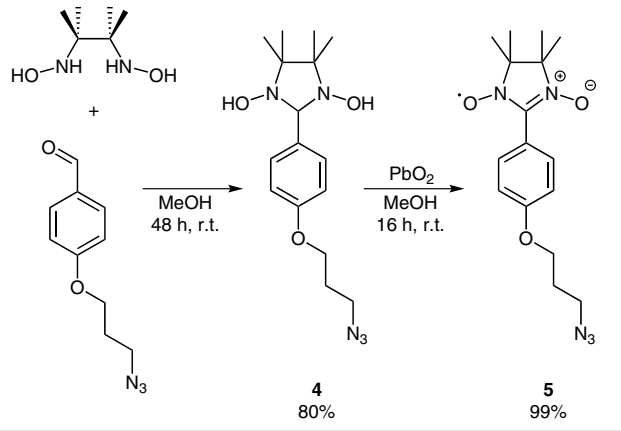

Scheme 1 Synthesis of azide-functionalized nitronyl nitroxide **5**

The structure of radical **5** was confirmed by mass spectrometry, elemental analysis, electron paramagnetic resonance (EPR) spectroscopy and by single-crystal X-ray diffraction. The EPR spectrum of **5** showed an isotropic five-line signal (Figure 2), which is expected for a nitronyl nitroxide type radical, and matches well with the simulated spectrum (Figure S3 in the Supporting Information). This confirms the presence of a radical in our sample, as well as proving that the radical is delocalized over two identical nitrogen atoms.

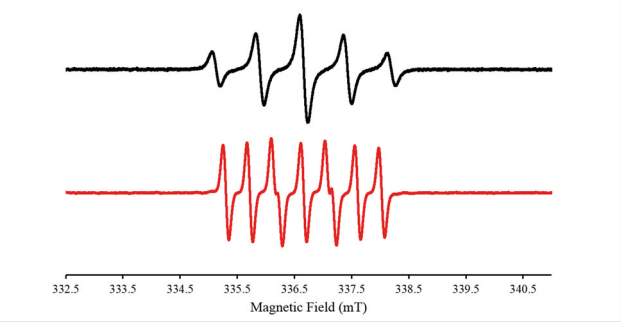

Figure 2 EPR spectrum of azide-substituted nitronyl nitroxide **5** (black) and azide-substituted imino nitroxide **7** (red) in CH_2Cl_2. Simulation parameters for **5**: linewidth = 0.09 mT, a_{N1} = 0.760 mT, g = 2.0075; and **7**: linewidth = 0.066 mT, a_{N1} = 0.910 mT, a_{N2} = 0.495 mT, g = 2.0472.

Single crystals that were suitable for X-ray diffraction studies were grown by cooling a concentrated pentane solution of **5**.[20] The solid-state structure confirmed the expected connectivity (Figure 3). The C1–N1 and C1–N2 bond lengths are identical, and fall between the expected bond lengths for a C–N single and double bond.[21] Similarly, the N1–O1 and N2–O2 bonds are the same length, and they are shorter than a typical N–OH bond (Table 1). This data confirms radical formation and delocalization.

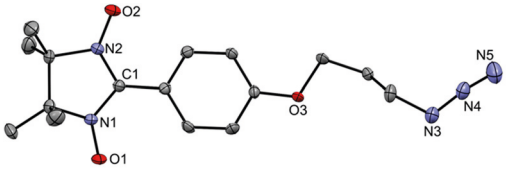

Figure 3 Solid-state structure of **5**; anisotropic displacement ellipsoids are shown at 50% probability and hydrogen atoms have been omitted for clarity.

Table 1 Selected Bond Lengths (Å) and Angles (°) for Nitronyl Nitroxide **5**

O1-N1, O2-N2	1.279(4), 1.281(4)
N1-C1, N2-C1	1.358(5), 1.351(5)
O1-N1-C1, O2-N2-C1	127.5(3), 126.1(3)
C2-N1-C1, C3-N2-C1	111.9(3), 111.8(3)
N1-C1-C8, N2-C1-C8	125.7(3), 126.4(4)

To explore the reactivity of **5** in the Staudinger–Bertozzi ligation reaction, we reacted it with the model molecule methyl-2-(diphenylphosphino)benzoate **6**, which was synthesized according to a published method.[22] The reaction was performed by stirring the components overnight in CH_2Cl_2 (Scheme 2). Interestingly, the major isolated product was orange rather than the expected dark-blue color of the azide-substituted nitronyl nitroxide radical **5**. This orange solid, which was isolated in 84% yield, was identified by mass spectrometry as imino nitroxide **7**. The transformation from nitronyl nitroxides to imino nitroxides has been shown to be facilitated by triphenylphosphines,[23] and results in the oxidation of triphenylphosphine to triphenylphosphine oxide (Scheme 2).

The EPR spectrum of the orange product was also consistent with the formation of an imino nitroxide radical, as the loss of symmetry in the molecule results in a seven-line signal (Figure S4 in the Supporting Information), which is very different from the five-line signal observed for nitronyl nitroxides (Figure 2). This experiment demonstrates that the reaction of nitronyl nitroxide **5** with **6** results mainly in the formation of imino nitroxide **7** in high yields.

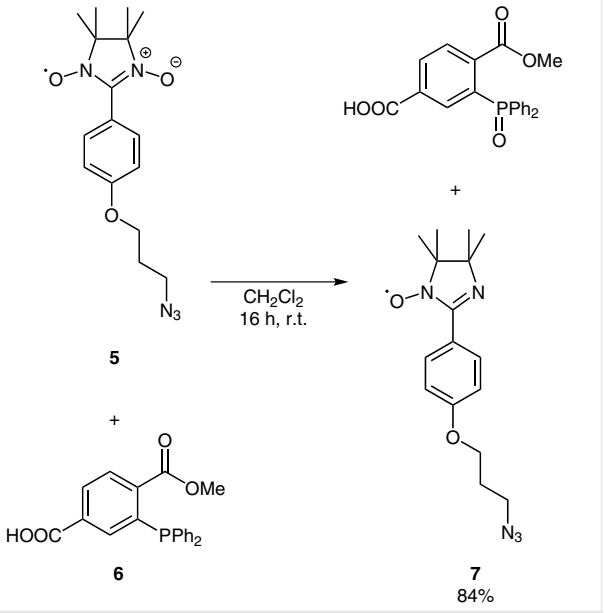

Scheme 2 Reaction resulting in the formation of imino nitroxide **7**

Interestingly, nitronyl nitroxide **5** showed different reactivity at the interface of gold nanoparticles. The azide-functionalized radical (ca. 200 equivalents) was reacted with nanoparticles displaying interfacial methyl-2-(diphenylphosphino)benzoate moieties (Staudinger-AuNP), which have been shown to react well with azide (bio)molecular systems.[24] The Staudinger-AuNP contain 0.432 μmol methyl-2-(diphenylphosphino)benzoate per milligram of nanoparticles. These AuNPs have an average nanoparticle raw formula of $Au_{1500}(MeO\text{-}EG_3\text{-}S)_{500}(Ph_3P\text{-}EG_4\text{-}S)_{200}(Ph_3P{=}O\text{-}EG_4\text{-}S)_{20}$, assuming that the AuNP are spherical and perfectly monodispersed in size (EG = $-CH_2CH_2O-$).[24]

The reaction between the Staudinger-AuNP and azide-substituted nitronyl nitroxide radical **5** was carried out by stirring the mixture in CH_2Cl_2 for 48 h. Subsequently, the excess radical was removed by settling the nanoparticles through centrifugation (6000 rpm, 10 min) and removing the mother liquor, using CH_2Cl_2–hexanes (1:6) as solvent. The particles, presumably due to the presence of the interfacial stable organic radical, lost their solubility in polar organic solvents. The remaining traces of **5** were removed by forming a film of AuNP inside a round-bottom flask and then rinsing it with hexanes followed by 95% ethanol. The cleaning procedure was monitored by IR spectroscopy, which was used to follow the disappearance of the azide peak of unreacted **5** at 2100 cm^{-1} (Figure S5 in the Supporting Information).

The purified radical-functionalized AuNP were first studied by transmission electron microscopy (TEM) to verify that the reaction with the radicals had not changed the size or shape of the nanoparticles. TEM images of the starting material, before reaction with the radical, showed that Staudinger-AuNP (3.6 ± 1.4 nm) self-assemble into islands. After the Staudinger–Bertozzi ligation with the azide-substituted nitronyl nitroxide radical, TEM images showed that the AuNPs retain the same size (3.1 ± 0.8 nm) and shape (Figure 4). The same images also show that the nanoparticles were well dispersed after the interfacial reaction. The tendency of the Staudinger-AuNP to form self-assemblies that disassemble upon reaction with azides is consistent with a previous report.[24]

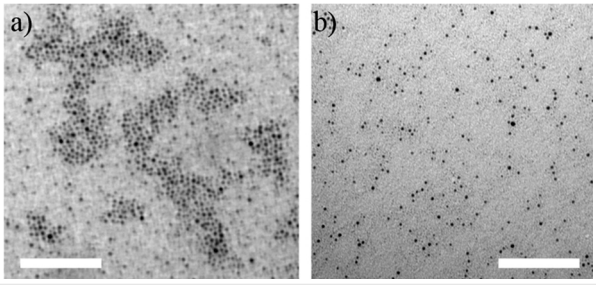

Figure 4 TEM images of (a) Staudinger–Bertozzi ligation particles and (b) radical-substituted gold nanoparticles (scale bars = 100 nm)

The EPR spectrum of the radical-functionalized AuNP showed a very similar pattern to that of unreacted radical **5**, a slightly anisotropic five-line signal (Figure 5), and is consistent with the simulated spectrum (Figure S6 in the Supporting Information). The anisotropy is likely derived from the fact that the radicals are unable to tumble freely in solution when appended to the nanoparticle. This result verified that the nitronyl nitroxide radical remains intact throughout the interfacial reaction with the nanoparticles, and covalently attached imino nitroxide radicals are not present. This difference in reactivity from solution is likely due to the difference in steric hindrance between the molecular system and the nanoparticles. The methyl-2-(diphenylphosphino)benzoate moieties appended to the nanoparticles are much more sterically hindered, and thus approach by the linear azide may be favored.

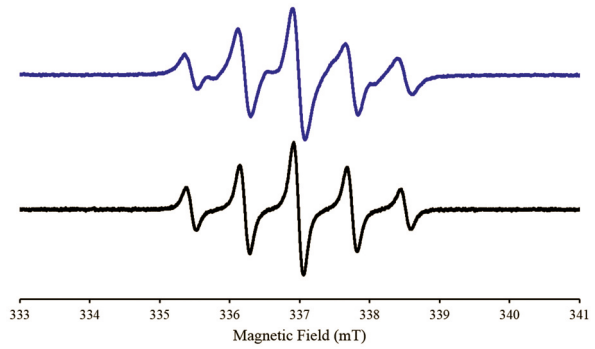

Figure 5 EPR spectra of radical-functionalized AuNPs (blue) and azide-functionalized nitronyl nitroxide **5** (black) in CH_2Cl_2. Simulation parameters for radical-functionalized AuNPs: linewidth = 0.16 mT, a_{N1} = 0.770 mT, g = 2.0068.

EPR spectroscopy was used to estimate the number of radicals present on the nanoparticles. By comparing the intensity of the EPR signal of the AuNP-radical sample with the intensity of a standard (TEMPO) solution, the number of unpaired electrons was estimated to be 7.5×10^{15} per milligram of sample (see the Supporting Information for full details), which corresponds to 1.25×10^{-2} µmol radical per milligram of sample.

The radical-functionalized AuNP were also characterized through X-ray photoelectron spectroscopy (XPS) and the results were compared to those of the starting material Staudinger-AuNP (Figure S7 in the Supporting Information).[24] High-resolution scans of the C 1s and of the P 2p corelines provide evidence of successful interfacial reactivity and allowed the amount of radical introduced onto the surface of the nanoparticle to be estimated. The C 1s peak after interfacial Staudinger–Bertozzi ligation showed a significant decrease in the component at 289.30 eV related to the carbonyl of the methyl ester functionality and a marked increase of the component at 288.00 eV due to the newly formed amide bonds between the methyl-2-(diphenylphosphino)benzoate and the azide-substituted nitronyl nitroxide radical. The P 2p coreline showed a marked increase in the triphenylphosphine oxide component. From the integration of the active triphenylphosphine component at 131.65 eV and the triphenylphosphine oxide component at 132.55 eV we calculated formation of 31% oxidized triphenylphosphine, taking into consideration that there is 10% phosphine oxide in the starting AuNP. Assuming that every moiety results from interfacial Staudinger–Bertozzi ligation with the radical, this percentage would correspond to approximately 0.133 µmol radical per milligram of nanoparticles. This number is different than the value calculated by EPR. The additional phosphine oxide arises from competing reactivity of the nitronyl nitroxide radical **5** with the Staudinger AuNP, to give imino nitroxide **7** in solution, which is removed through washing. This explains the excess phosphine oxide observed through XPS. However, EPR spectroscopy confirmed unambiguously that the *ligated* radical is a nitronyl nitroxide.

An important control experiment to verify the correct interfacial reactivity between Staudinger-AuNP and radical **5** and the absence of unspecific binding was also performed. For this experiment, radical **5** was stirred for 48 h in CH_2Cl_2 with triethylene glycol-monomethyl ether AuNP starting material (TEG-AuNP) that does not possess the interfacial methyl-2-(diphenylphosphino)benzoate moieties. Because of the absence of unspecific interaction between the radicals and the nanoparticles, the solubility properties of the TEG-AuNP did not change and, therefore, it was necessary to adopt a different cleaning procedure. The excess radical was removed by forming a AuNP film inside a round-bottom flask from CH_2Cl_2, and washing with hexanes. Remaining traces of radical were removed by dissolving the TEG-AuNP in water and by filtering the insoluble radical through glass-wool. The successful removal of the azide-functionalized nitronyl nitroxide radical was monitored by IR spectroscopy as before (Figure S8 in the Supporting Information). The EPR spectrum of the control experiment carried out using these nanoparticles (Figure S9 in the Supporting Information) showed, as expected, no signal, and thus we can conclude that the azide-functionalized radical reacts selectively with the triphenylphosphine moiety through Staudinger–Bertozzi ligation, and that there are no radicals bound to AuNP through any other bonding modes.

In conclusion, we have demonstrated the straightforward synthesis of the first azide-substituted nitronyl nitroxide radical. The reactivity of this radical with modified triphenylphosphines for use in Staudinger–Bertozzi ligation was also examined. The reactivity of the radical differed between the nanoparticle system (AuNP) and a small molecule model system. Whereas in the model system, formation of an imino nitroxide was observed as the major product, we were able to observe the expected ligation product between the azide-functionalized nitronyl nitroxide and Staudinger–Bertozzi AuNP. The combination of EPR spectroscopy and XPS allowed us to demonstrate successful interfacial reactivity and to estimate the number of nitronyl nitroxide radicals that were present in the nanoparticle sample. Furthermore, we believe that the approach described here can be easily transposed to other nanomaterials with potential application, for example, as solid-supported catalysts, contrasting agents, and spin-labels.

Acknowledgment

The authors thank the Natural Sciences and Engineering Research Council (NSERC) of Canada Discovery Grants (J.B.G. and M.S.W.), Canada Graduate Scholarship (S.M.B.), Vanier Graduate Scholarship (P.G.) and OGS (W.L.) programs, a Petro-Canada Young Innovator Award (J.B.G.) and The University of Western Ontario for financial support. We also thank Prof. Giovanni Fanchini for access to his EPR spectrometer.

Supporting Information

Supporting information for this article is available online at http://dx.doi.org/10.1055/s-0035-1560707.

Primary Data

Primary data for this article are available online at http://www.thieme-connect.com/products/ejournals/journal/10.1055/s-00000083 and can be cited using the following DOI: 10.4125/pd0072th.

References and Notes

(1) These authors contributed equally to this work.
(2) Gomberg, M. *J. Am. Chem. Soc.* **1900**, *22*, 757.
(3) *Stable Radicals: Fundamentals and Applied Aspects of Odd-Electron Compounds*; Hicks, R. G., Ed.; Wiley: West Sussex, **2010**.
(4) (a) Rajca, A.; Wongsriratanakul, J.; Rajca, S. *Science* **2001**, *294*, 1503. (b) Winter, S. M.; Hill, S.; Oakley, R. T. *J. Am. Chem. Soc.* **2015**, *137*, 3720.
(5) (a) Rajca, A.; Wang, Y.; Boska, M.; Paletta, J. T.; Olankitwanit, A.; Swanson, M. A.; Mitchell, D. G.; Eaton, S. S.; Eaton, G. R.; Rajca, S. *J. Am. Chem. Soc.* **2012**, *134*, 15724. (b) Huang, L.; Yan, C.; Cui, D.; Yan, Y.; Liu, X.; Lu, X.; Tan, X.; Lu, X.; Xu, J.; Xu, Y.; Liu, R. *Macromol. Biosci.* **2015**, *15*, 788.
(6) (a) Nishide, H.; Oyaizu, K. *Science* **2008**, *319*, 737. (b) Janoschka, T.; Hager, M. D.; Schubert, U. S. *Adv. Mater.* **2012**, *24*, 6397.
(7) (a) Adam, W.; Saha-Möller, C. R.; Ganeshpure, P. A. *Chem. Rev.* **2001**, *101*, 3499. (b) Vogler, T.; Studer, A. *Synthesis* **2008**, 1979.
(8) (a) Samuni, A.; Goldstein, S.; Russo, A.; Mitchell, J. B.; Krishna, M. C.; Neta, P. *J. Am. Chem. Soc.* **2002**, *124*, 8719. (b) Damiani, E.; Castagna, R.; Astolfi, P.; Greci, L. *Free Rad. Res.* **2005**, *39*, 325.
(9) (a) Wright, P. J.; English, A. M. *J. Am. Chem. Soc.* **2003**, *125*, 8655. (b) Lam, M. A.; Pattison, D. I.; Bottle, S. E.; Keddie, D. J.; Davies, M. J. *Chem. Res. Toxicol.* **2008**, *21*, 2111. (c) Zhang, J.; Zhao, M.; Cui, G.; Peng, S. *Bioorg. Med. Chem.* **2008**, *16*, 4019.
(10) (a) Krishna, M. C.; DeGraff, W.; Hankovszky, O. H.; Sár, C. P.; Kálai, T.; Jekő, J.; Russo, A.; Mitchell, J. B.; Hideg, K. *J. Med. Chem.* **1998**, *41*, 3477. (b) Hoye, A. T.; Davoren, J. E.; Wipf, P.; Fink, M. P.; Kagan, V. E. *Acc. Chem. Res.* **2008**, *41*, 87.
(11) (a) Konorev, E. A.; Tarpey, M. M.; Joseph, J.; Baker, J. E.; Kalyanaraman, B. *Free Radical Biol. Med.* **1995**, *18*, 169. (b) Rosen, G. M.; Porasuphatana, S.; Tsai, P.; Ambulos, N. P.; Galtsev, V. E.; Ichikawa, K.; Halpern, H. J. *Macromolecules* **2003**, *36*, 1021.
(12) (a) Fischer, H. *Chem. Rev.* **2001**, *101*, 3581. (b) Hawker, C. J.; Bosman, A. W.; Harth, E. *Chem. Rev.* **2001**, *101*, 3661. (c) Sciannamea, V.; Jérôme, R.; Detrembleur, C. *Chem. Rev.* **2008**, *108*, 1104.
(13) Berliner, L. J. *Spin Labeling: A Modern Perspective*, In *Stable Radicals: Fundamentals and Applied Aspects of Odd-Electron Compounds*; Hicks, R. G., Ed.; Wiley: West Sussex, **2010**, 521–536.
(14) (a) Swiech, O.; Hrynkiewicz-Sudnik, N.; Palys, B.; Kaim, A.; Bilewicz, R. *J. Phys. Chem. C* **2011**, *115*, 7347. (b) Garbuio, L.; Antonello, S.; Guryanov, I.; Li, Y.; Ruzzi, M.; Turro, N. J.; Maran, F. *J. Am. Chem. Soc.* **2012**, *134*, 10628. (c) Boccalon, M.; Franchi, P.; Lucarini, M.; Delgado, J. J.; Sousa, F.; Stellacci, F.; Zucca, I.; Scotti, A.; Spreafico, R.; Pengo, P.; Pasquato, L. *Chem. Commun.* **2013**, *49*, 8794. (d) Swiech, O.; Bilewicz, R.; Megiel, E. *RSC Adv.* **2013**, *3*, 5979.
(15) Krim, J.; Taourirte, M.; Grünewald, C.; Krstic, I.; Engels, J. W. *Synthesis* **2013**, *45*, 396.
(16) (a) Kálai, T.; Hubbell, W. L.; Hideg, K. *Synthesis* **2009**, 1336. (b) Jakobsen, U.; Shelke, S. A.; Vogel, S.; Sigurdsson, S. T. *J. Am. Chem. Soc.* **2010**, *132*, 10424.
(17) Yilmaz, M. D.; Bozdemir, O. A.; Akkaya, E. U. *Org. Lett.* **2006**, *8*, 2871.
(18) Shimono, S.; Tamura, R.; Ikuma, N.; Takimoto, T.; Kawame, N.; Tamada, O.; Sakai, N.; Matsuura, H.; Yamauchi, J. *J. Org. Chem.* **2004**, *69*, 475.
(19) **Preparation of Azide-Functionalized Nitronyl Nitroxide 5**: Imidazoline **4** (2.00 g, 5.96 mmol) and lead oxide (4.28 g, 17.9 mmol) were mixed in methanol (50 mL). A blue color formed almost immediately. The reaction was stirred for 16 h before it was filtered and concentrated in vacuo to give a dark-blue residue. Nitronyl nitroxide **5** was purified by filtration through a small plug of neutral alumina with CH_2Cl_2 to give a dark-blue microcrystalline solid. Yield: 1.96 g (99%); mp 74–76 °C. FTIR (KBr): 3090 (m), 2992 (s), 2938 (s), 2881 (s), 2553 (w), 2096 (s), 1606 (s), 1572 (m), 1531 (m) cm^{-1}. UV/Vis (CH_2Cl_2): λ_{max} (ε, $M^{-1}cm^{-1}$) = 622 (1,100), 368 (13,900), 285 (22,900) nm. HRMS (EI, +ve mode): *m*/*z* calcd for $[C_{16}H_{22}N_5O_3]^+$: 332.1723; found: 332.1721 (diff.: –0.45 ppm). Anal. Calcd (%) for $C_{16}H_{22}N_5O_3$: C, 57.82; H, 6.67; N, 21.07. Found: C, 58.09; H, 6.76; N, 21.01.
(20) Crystallographic data for **5** has been deposited into the Cambridge Crystallographic Data Centre with the deposition number CCDC-1414896 and is also available in the primary data file associated with this manuscript.
(21) *CRC Handbook of Chemistry and Physics*; Haynes, W. M., Ed.; CRC Press: Boca Raton, Fla, **2012**.
(22) Wang, C. C.-Y.; Seo, T. S.; Li, Z.; Ruparel, H.; Ju, J. *Bioconjugate Chem.* **2003**, *14*, 697.
(23) Ullman, E. F.; Call, L.; Osiecki, J. H. *J. Org. Chem.* **1970**, *35*, 3623.
(24) Gobbo, P.; Luo, W.; Cho, S. J.; Wang, X.; Biesinger, M. C.; Hudson, R. H. E.; Workentin, M. S. *Org. Biomol. Chem.* **2015**, *13*, 4605.